

# Biologically Inspired and Magnetically Recoverable Copper Porphyrinic Catalysts: A Greener Approach for Oxidation of Hydrocarbons with Molecular Oxygen

César A. Henriques, Auguste Fernandes, Liane M. Rossi, M. Filipa Ribeiro, Mário J. F. Calvete,\* and Mariette M. Pereira\*

An efficient synthetic method for magnetically recoverable hybrid copper porphyrinic nanomaterials is reported. These functionalized magnetic materials prove to be efficient bioinspired oxidation catalysts of olefins and thiols, using molecular oxygen as oxidant, in total absence of reductants and solvents, with the highest TON (turnover number) yet achieved for this reaction ( $\approx 200\,000$ ). A comparative study between homogeneous and heterogeneous oxidation of cyclohexene is discussed, revealing the heterogeneous system to be the most promising concerning stability and reusability of the catalysts. The full characterization of the magnetic hybrid porphyrinic nanomaterials, by transmission electron microscopy, flame atomic absorption spectrometry, thermogravimetry,  $N_2$  sorption, and infrared spectroscopy, is also described.

## 1. Introduction

As the isolation of natural cytochrome-P450 monooxygenase enzymes (bearing iron(III)-protoporphyrin-IX as prosthetic group) is a quite difficult task,<sup>[1–3]</sup> the use of synthetically modulated metalloporphyrins has been a great challenge for chemists,<sup>[4,5]</sup> not only for the understanding of natural systems<sup>[6,7]</sup> but also for developing new highly efficient homogeneous<sup>[4,8–12]</sup> or heterogeneous oxidation catalysts,<sup>[12–15]</sup> particularly the ones involving the use of nonpolluting oxygen

donors such as molecular oxygen<sup>[16–18]</sup> or hydrogen peroxide.<sup>[19–22]</sup> The major challenge in mimicking cytochrome-P450 enzymes is the development of catalytic systems capable to promote the insertion of one oxygen atom from  $O_2$  on the substrate and also the two electron reduction of the other oxygen atom to water (in nature this process is carried out by NAD(P)H reductase protein).<sup>[4]</sup> To overcome this issue, the addition of several reductants such as zinc dust or aldehydes<sup>[23–25]</sup> to the metalloporphyrins oxidation catalytic systems or use of high temperatures and pressures<sup>[26–29]</sup> have been reported. Few other examples have been described in the literature on the

use of metalloporphyrins as catalysts for olefin oxidation using  $O_2$  as oxidant in absence of coreductants,<sup>[30–33]</sup> though demonstrating relatively low catalytic activity. However, it should be noted that the transformation of metalloporphyrins as valuable oxidation catalysts for large scale purposes is still a challenging endeavor, mainly due to issues related to porphyrin stability, cost and reutilization.<sup>[34]</sup> The envisaged solution relies on the development of efficient procedures for the immobilization of porphyrins into/onto solid supports,<sup>[13–15]</sup> namely, mesoporous aluminosilicates,<sup>[35,36]</sup> polymers<sup>[37–40]</sup> and double-layered hydroxides,<sup>[41,42]</sup> nevertheless generally requiring the use of polluting oxidants and  $O_2$  with coreductants. Beyond these strategies, magnetic nanoparticles have recently revealed promising properties concerning both catalytic activity and reusability.<sup>[43,44]</sup> Among them, there are just few examples on the application of porphyrin based magnetic catalysts for oxidation reactions, using either polluting oxidation agents<sup>[45–47]</sup> or  $H_2O_2$ .<sup>[48]</sup>

This paper describes an efficient synthetic method for porphyrins bearing appropriate functional groups to promote their linkage to selectively functionalized magnetic nanoparticles and its full characterization by transmission electron microscopy, flame atomic absorption spectrometry, thermogravimetry,  $N_2$  sorption, and infrared spectroscopy. The new hybrid magnetic nanomaterials were evaluated as reusable biomimetic catalysts in hydrocarbon oxidation reactions (cyclohexene,  $\alpha$ -pinene,  $\beta$ -pinene, and thiophenol), using molecular oxygen, in total absence of reductants and solvents.

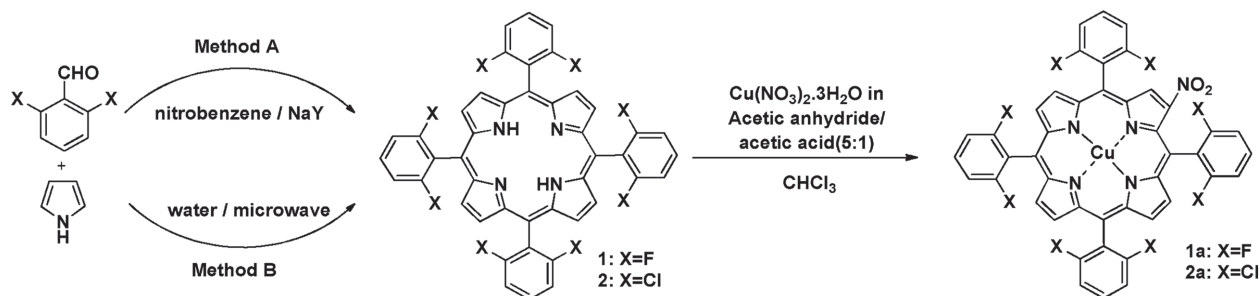
C. A. Henriques, Dr. M. J. F. Calvete,  
Prof. M. M. Pereira  
CQC  
Department of Chemistry  
University of Coimbra  
Rua Larga, 3004-535 Coimbra, Portugal  
E-mail: mcalvete@qui.uc.pt; mmpereira@qui.uc.pt

Dr. A. Fernandes, Prof. M. F. Ribeiro  
Centro de Química Estrutural  
Instituto Superior Técnico  
Universidade de Lisboa  
Av. Rovisco Pais, 1049-001 Lisboa, Portugal

Prof. L. M. Rossi  
Departamento de Química Fundamental  
Instituto de Química  
Universidade de São Paulo  
Av. Prof. Lineu Prestes 748 sl. 1256, 05508-000 São Paulo, SP, Brasil



DOI: 10.1002/adfm.201505405



Scheme 1. Metalloporphyrin synthesis.

## 2. Results and Discussion

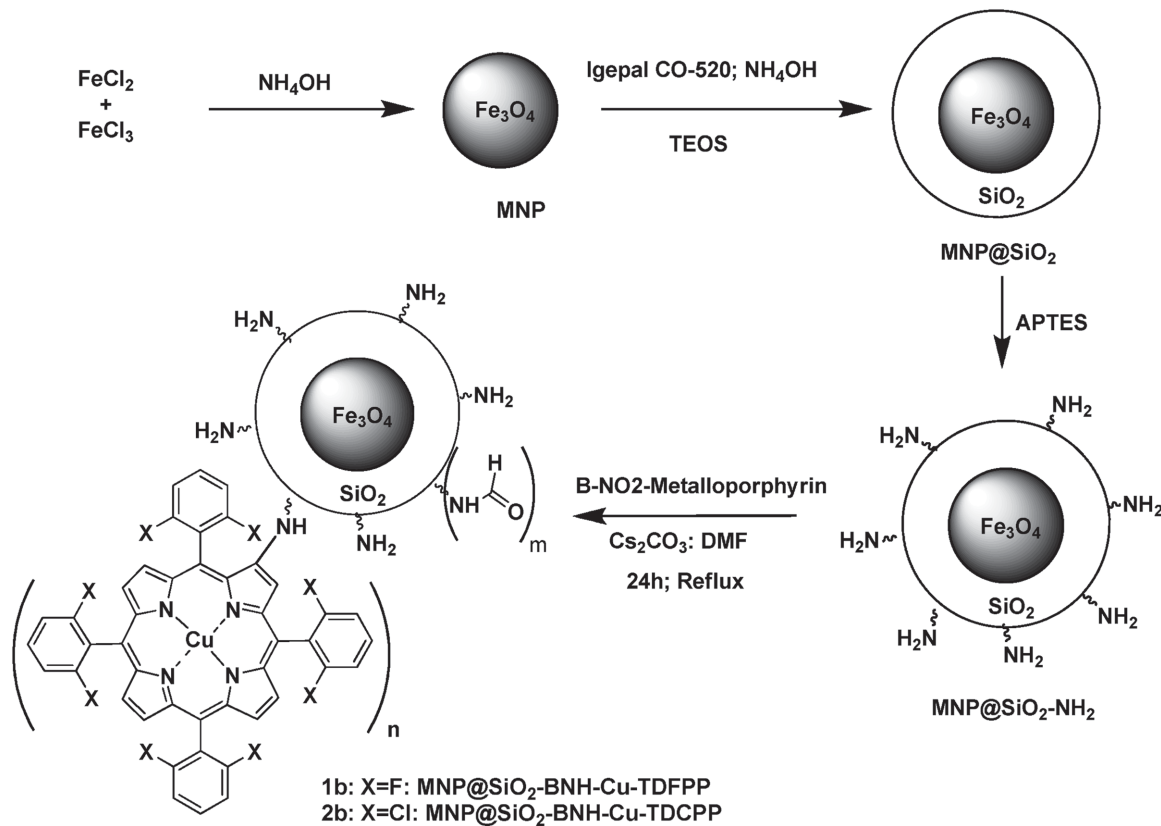
### 2.1. Synthesis and Characterization of the Catalysts

The halogenated *meso*-tetraarylporphyrins **1** and **2** were synthesized through one-pot condensation of pyrrole and the corresponding 2,6-difluorobenzaldehyde or 2,6-dichlorobenzaldehyde using our recently reported nitrobenzene/NaY method<sup>[49]</sup> (Scheme 1, method A) or preferentially the more sustainable water/microwave method<sup>[50,51]</sup> (Scheme 1, method B). While method B afforded porphyrins **1** and **2** in 21% and 7.5% yields, respectively, method A gave the same porphyrins **1** and **2** in 9% and 3% yields, respectively.

Subsequent  $\beta$ -mononitration and copper complex formation for each porphyrin was carried out by mixing the desired

halogenated porphyrin with copper nitrate trihydrate (two equivalents) in a solution of acetic anhydride/acetic acid (5:1).<sup>[52]</sup> After optimization of reaction conditions the copper(II) 2-nitro-5,10,15,20-tetra(2,6-difluorophenyl)porphyrinate (**1a**) and copper(II) 2-nitro-5,10,15,20-tetra(2,6-dichlorophenyl)porphyrinate (**2a**) were obtained in 89% and 76% yield, respectively.

In order to prepare the hybrid magnetic materials, first we promoted the synthesis of the magnetic cores by coprecipitation of  $\text{Fe}^{2+}/\text{Fe}^{3+}$  ions under alkaline conditions, followed by stabilization with oleic acid according to previously reported methodology<sup>[53]</sup> (MNP, magnetic nanoparticles) (Scheme 2). Transmission electron microscopy (TEM) images of the oleic acid stabilized MNP display a diameter size distribution of  $8.3 \pm 2.4$  nm (Figure S1, Supporting Information). Finally, the MNP were reacted with tetraethylorthosilicate (TEOS) and



Scheme 2. Preparation and functionalization of magnetic nanoparticles by covalent linking.

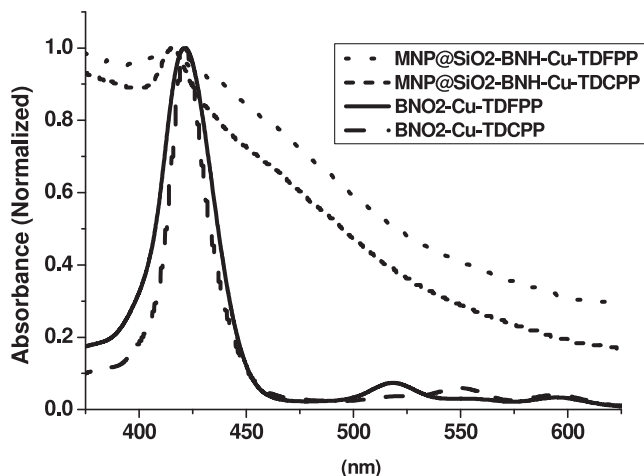


**Figure 1.** Absorption spectra of  $\beta\text{NO}_2\text{-Cu-TDFPP}$  (**1a**) and  $\beta\text{NO}_2\text{-Cu-TDCPP}$  (**2a**) in  $\text{CHCl}_3$  and  $\text{MNP@SiO}_2\text{-BNH-Cu-TDFPP}$  (**1b**) and  $\text{MNP@SiO}_2\text{-BNH-Cu-TDCPP}$  (**2b**) in acetonitrile:water (1:1).

a uniform layer of silica was deposited on the iron oxide surfaces<sup>[54]</sup> ( $\text{MNP@SiO}_2$ ) (Scheme 2). The particle size distribution was obtained by TEM and, as expected, a size increase to  $28.9 \pm 5.1$  nm was observed, when compared with MNP (Figure S2, Supporting Information).

To promote the covalent anchoring of  $\text{BNO}_2\text{-Cu-TDFPP}$  (**1a**) and  $\text{BNO}_2\text{-Cu-TDCPP}$  (**2a**), the  $\text{MNP@SiO}_2$  was previously amino-functionalized, by reaction with 3-aminopropyltriethoxysilane (APTES), in dry toluene, providing the aminopropyl-modified magnetic nanoparticles ( $\text{MNP@SiO}_2\text{-NH}_2$ ) (Scheme 2). Then, reaction of  $\text{MNP@SiO}_2\text{-NH}_2$  with  $\beta$ -nitro metalloporphyrins **1a** and **2a** was carried out using dry *N,N*-dimethylformamide (DMF) as solvent, at 423 K (150 °C), along 24 h, yielding  $\text{MNP@SiO}_2\text{-BNH-Cu-TDFPP}$  (**1b**) and  $\text{MNP@SiO}_2\text{-BNH-Cu-TDCPP}$  (**2b**) after washing several times with acetonitrile, ethyl acetate, and dichloromethane, to rinse away excess of unreacted metalloporphyrin. Additionally, it is known that DMF can act as amine formylating agent, in presence of bases, when the reaction is carried out at refluxing temperatures.<sup>[55]</sup> Therefore, in order to accurately determine the degree of  $\text{MNP@SiO}_2\text{-NH}_2$  functionalization, we have performed an additional experiment in which the amine functionalized silica coated magnetic nanoparticle reacted with DMF, in presence of  $\text{Cs}_2\text{CO}_3$ , at refluxing temperatures and the resulting materials were characterized by TG/DSC and IR (see Figures S3 and S4, Supporting Information).

Moreover, the copper porphyrinic hybrid magnetic nanoparticles **1b** and **2b** were characterized by UV-vis spectroscopy (Figure 1), whose absorption spectra show the typical Soret bands of porphyrinic type molecules at 420 nm. The amount of copper on the magnetic nanoparticles was determined by flame atomic absorption spectroscopy (FAAS), showing the presence of 0.1% Cu in **1b** and 0.03% Cu in **2b**, which is indicative of the presence of 1.3% ( $0.015 \text{ mmol g}^{-1}$ ) and 0.5% ( $0.0051 \text{ mmol g}^{-1}$ ) of metalloporphyrins **1a** and **2a**, respectively.

### 2.1.1. Thermogravimetric Analysis

In order to quantify the organic content for all nanocomposite materials, thermogravimetry/differential scanning calorimetry (TG/DSC) measurements in the range between room temperature and 1073 K (800 °C) were carried out (Figure 2a–e).

One endothermic peak between 323 and 423 K (50 and 150 °C) was observed for all samples, with weight loss corresponding to physically adsorbed water. A weight loss of 4.0% was observed for aminopropyl functionalized  $\text{MNP@SiO}_2\text{-NH}_2$ , which was attributed to decomposition of the aminopropyl groups grafted at the surface of the  $\text{MNP@SiO}_2$  matrix (1.1% of  $\text{NH}_2$  corresponding to  $0.68 \text{ mmol g}^{-1}$ ) (Figure 2a).

In the TG/DSC analysis from metalloporphyrins **1a**, **2a** (Figure 2b,c respectively), decomposition between 673 and 923 K (400 and 650 °C) could be observed. Since  $\text{MNP@SiO}_2\text{-N-formyl}$  decomposes essentially up to 673 K (400 °C) (see Figure S1, Supporting Information), weight losses occurring in the temperature range 673–923 K (400–650 °C) for samples **1b** and **2b** can be considered to arise essentially from metalloporphyrins **1a** and **2a** adsorbed to  $\text{MNP@SiO}_2\text{-NH}_2$ . The TG/DSC curves of **1b** and **2b** (Figure 2d,e, respectively) showed a weight loss of 1.2% and 0.7%, respectively, due to metalloporphyrin decomposition. The amount of metalloporphyrins **1a** and **2a** grafted onto magnetic nanoparticles was calculated as 0.015 and 0.007 mmol per gram of  $\text{MNP@SiO}_2$ , respectively, which is in agreement with the values obtained by flame atomic absorption spectroscopy technique.

### 2.1.2. Infrared Spectroscopy

Moreover, in situ infrared spectroscopy (FTIR) was also used to characterize the magnetic nanomaterials. The spectra of  $\text{MNP@SiO}_2$  (a),  $\text{MNP@SiO}_2\text{-NH}_2$  (b), **1b** (c), and **2b** (d) are presented in Figure 3.

The spectrum of  $\text{MNP@SiO}_2$  functionalized with aminopropyl shows peaks at 3371, 3309, and  $1597 \text{ cm}^{-1}$  (respectively, antisymmetric, symmetric stretching, and bending of  $\text{NH}_2$ );  $2931\text{--}2865$  and  $1450 \text{ cm}^{-1}$  (respectively, stretching and bending of  $\text{CH}_2$ ) and  $1410 \text{ cm}^{-1}$  characteristic of Si- $\text{CH}_2$  bending vibration. Also a narrow band, appearing at about  $3740 \text{ cm}^{-1}$  in the spectrum of raw silica-coated MNP material disappears with aminopropyl functionalization, probably due to the consumption of the silanol groups present at the surface of the material. After metalloporphyrins covalent grafting in DMF, the bands at about 3371, 3309, and  $1597 \text{ cm}^{-1}$  assigned to  $\text{NH}_2$  stretching and scissoring disappear completely. Concomitantly, some of the unreacted amine groups were converted to N-formyl groups by reaction with DMF,<sup>[55]</sup> leading to the appearance of bands at 1674, 1582, and  $1386 \text{ cm}^{-1}$  corresponding to C=O, N-H bending and C-N stretching, respectively (see Figure S4, Supporting Information). On the other hand, a new band, characteristic of aromatic CH groups stretching of metalloporphyrins, appears at  $3150\text{--}3050 \text{ cm}^{-1}$  which corroborates the immobilization of the metalloporphyrins to the magnetic nanoparticle coated with silica.<sup>[45–48]</sup> Additionally, the IR spectrum of  $\text{MNP@SiO}_2\text{-BNH-Cu-TDFPP}$  (d) also shows the typical metalloporphyrin **1a** peaks at 1625, 1585, and  $1465 \text{ cm}^{-1}$  (Figure S5, Supporting Information).

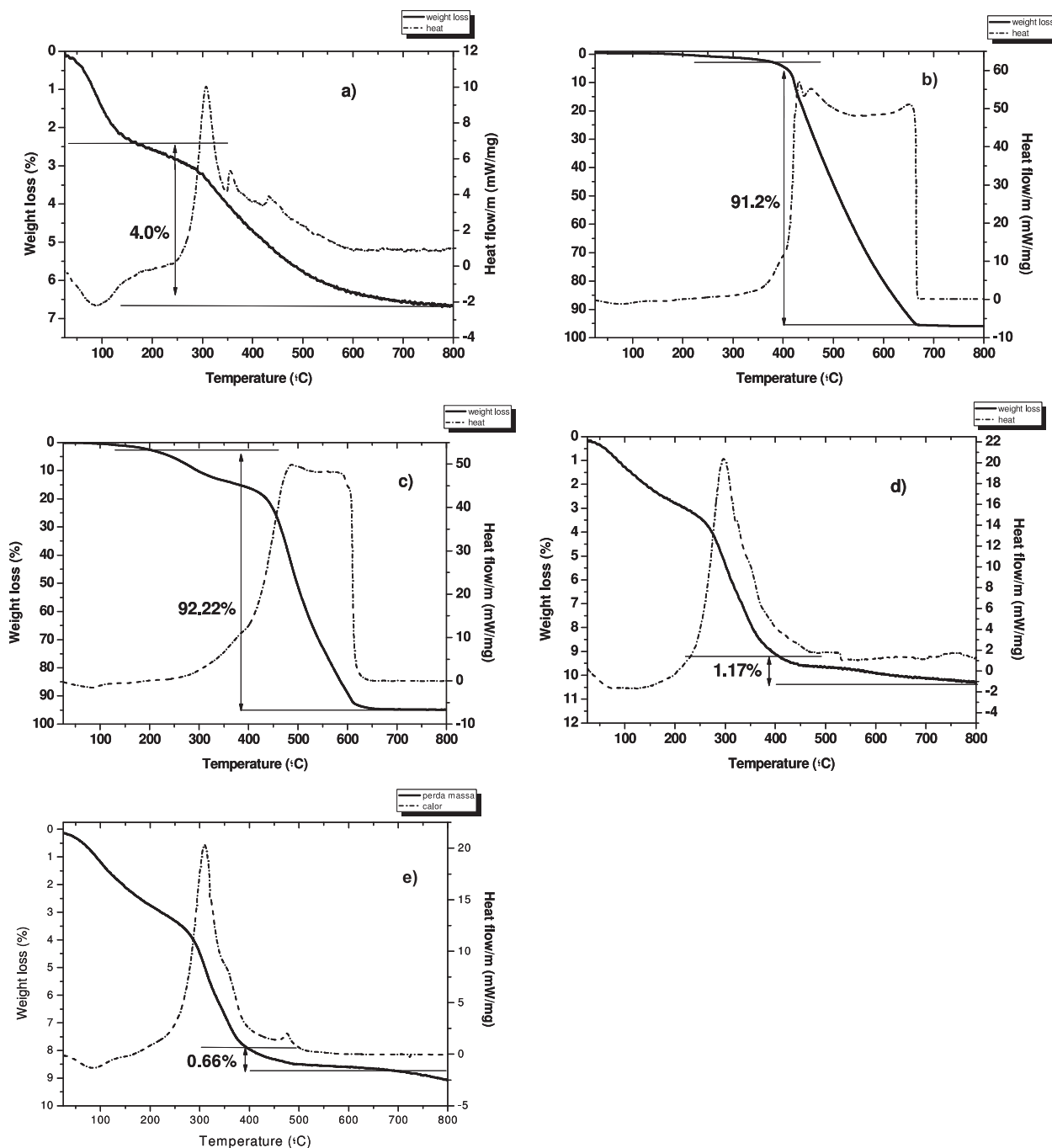


**Figure 2.** TG/DSC curves (heat dashed line, weight loss solid line): a) MNP@SiO<sub>2</sub>-NH<sub>2</sub>, b) **1a**, c) **2a**; d) **1b**; e) **2b**.

### 2.1.3. N<sub>2</sub> Sorption

The immobilization of the aminopropyl and metalloporphyrins on silica-coated magnetic nanoparticles (MNP@SiO<sub>2</sub>) expectedly affected their surface area. MNP@SiO<sub>2</sub> exhibited a specific area of 107 m<sup>2</sup> g<sup>-1</sup>, which decreased to 91 m<sup>2</sup> g<sup>-1</sup> after aminopropyl functionalization (Table S1, Supporting Information). Upon immobilization of metalloporphyrins **1a** or **2a** the specific areas decreased to 65 and 72 m<sup>2</sup> g<sup>-1</sup>, respectively. These values are in agreement with values obtained from

TG/DSC and FAAS, demonstrating that a higher quantity of BNO<sub>2</sub>-Cu-TDFPP **1a** than BNO<sub>2</sub>-Cu-TDCPP **2a** was immobilized on the magnetic nanoparticles. Also, the C parameter (which measures the affinity of the adsorbate for the surface) is in agreement to the synthetic procedure shown in Scheme 2, as MNP@SiO<sub>2</sub> presents a relatively high parameter C typical of mesoporous silica, which decreases upon organic group coating (Table S1, Supporting Information).

Regarding N<sub>2</sub> sorption measurements, all materials show a type IV isotherms profile (as defined by IUPAC classification)

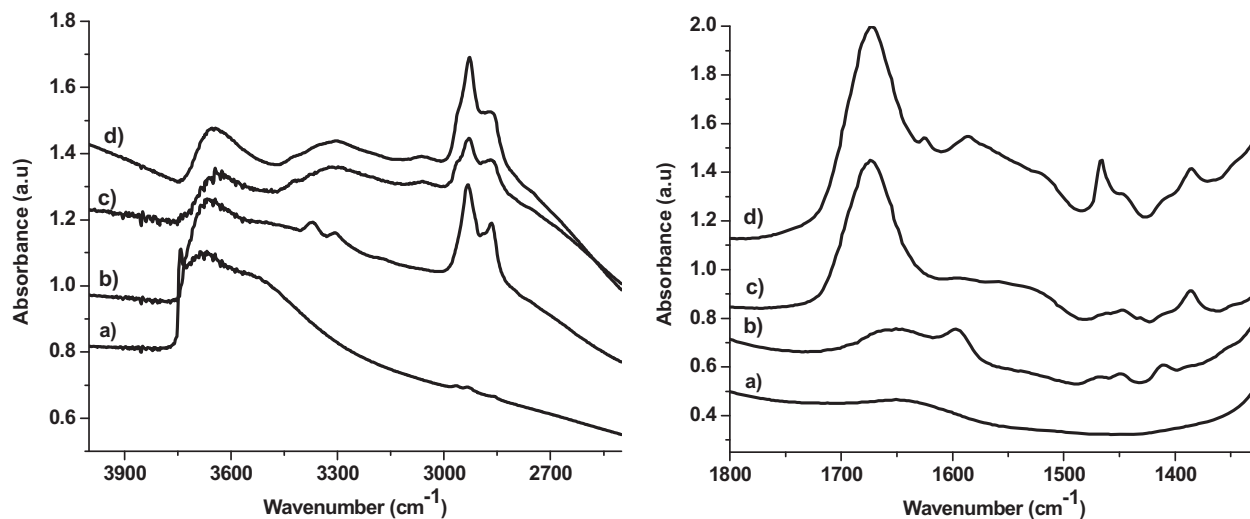


**Figure 3.** Infrared spectra of a) MNP@SiO<sub>2</sub>, b) MNP@SiO<sub>2</sub>-NH<sub>2</sub>, c) MNP@SiO<sub>2</sub>-BNH-Cu-TDCPP, and d) MNP@SiO<sub>2</sub>-BNH-Cu-TDFPP. (Left) IR region 4000–2500 cm<sup>-1</sup> and (right) IR region 1800–1325 cm<sup>-1</sup>.

with a H<sub>2</sub> hysteresis, typical for amorphous silica-gel materials (Figure S7, Supporting Information). The existence of a hysteresis is probably due to the presence of nanoparticles with interparticular voids in the range of mesopores. We may conclude that the textural properties of magnetic nanoparticles coated with silica samples were substantially maintained after the metalloporphyrin complex immobilization.

### 3. Oxidative Catalytic Experiments

#### 3.1. Catalytic Experiments

Cyclohexene was selected as a model substrate to optimize the conditions for homogeneous and heterogeneous oxidation processes using metalloporphyrins and the magnetic recoverable nanomaterials thereof as catalysts and molecular oxygen as oxidant. In a typical homogeneous oxidation experiment, a glass

reactor was loaded with the appropriate amount of cyclohexene and the desired metalloporphyrin **1a** and **2a**. The solution was magnetically stirred at 373 K (100 °C) under 400 kPa of O<sub>2</sub> pressure for the appropriate time. Substrate conversion and reaction selectivity was evaluated by GC and/or GC-MS, with aliquots taken from the reactor, after cooling down to room temperature and depressurization. First, the effect of the substrate/catalyst (S/C) molar ratio (500 to 500 000) was evaluated using BNO<sub>2</sub>-Cu-TDCPP **2a** as catalysts and the results of conversion and selectivity are presented in Table 1.

From the analysis of Table 1, one can conclude that the main products are 2-cyclohexen-1-one and 2-cyclohexen-1-ol, which may be attributed to the preferential cyclohexene allylic oxidation.<sup>[56–59]</sup> The selectivity toward the preferential formation of 2-cyclohexen-1-one versus 2-cyclohexen-1-ol is clearly dependent on the S/C molar ratio. At S/C = 5000, 2-cyclohexen-1-one is the main product formed (61%) (Table 1, entry 3), while increasing the S/C molar ratio caused a decreased in the

**Table 1.** Cyclohexene oxidation products using BNO<sub>2</sub>-Cu-TDCPP (**2a**) as catalyst and O<sub>2</sub> as oxidant.

| Entry | S/C <sup>a)</sup> | Conv. <sup>b)</sup> [%] | TON <sup>c)</sup> | Products selectivity <sup>d)</sup> [%] |    |    |                      |
|-------|-------------------|-------------------------|-------------------|--|----|----|----------------------|
|       |                   |                         |                   | 1                                      | 2  | 3  | Others <sup>e)</sup> |
| 1     | 500               | 66                      | 305               | 0                                      | 69 | 21 | 10                   |
| 2     | 1000              | 55                      | 550               | 0                                      | 61 | 29 | 10                   |
| 3     | 5000              | 56                      | 2793              | 0                                      | 61 | 28 | 11                   |
| 4     | 50 000            | 39                      | 19 599            | 6                                      | 32 | 40 | 22                   |
| 5     | 500 000           | 40                      | 201 015           | 8                                      | 42 | 37 | 13                   |

<sup>a)</sup>S/C = substrate to catalyst molar ratio; <sup>b)</sup>Conditions reactions: cyclohexene (10 mL, 0.099 mol), 373 K (100 °C); 400 kPa O<sub>2</sub>, 4 h; <sup>c)</sup>TON = turnover number = the number of moles of catalyst used per number of moles substrate converted; <sup>d)</sup>Determined by GC; <sup>e)</sup>Mass balance.

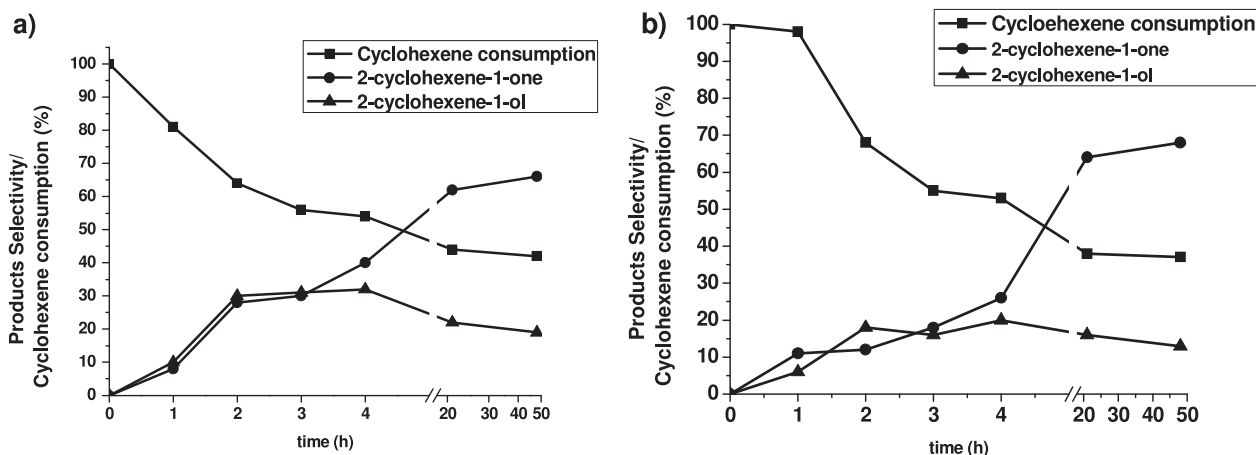


**Figure 4.** Cyclohexene conversion using  $O_2$  (400 KPa) as oxidant and a)  $BNO_2$ -TDFPP **1a** or b)  $BNO_2$ -TDCPP **2a** as catalysts (followed by GC-MS).

ketone formation and a clear accumulation of 2-cyclohexene-1-ol (Table 1, entries 4 and 5). These results indicate that the rate of 2-cyclohexene-1-ol oxidation toward the corresponding ketone depends on the S/C molar ratio; nonetheless cyclohexene allylic oxidation seems to be the preferential pathway. Furthermore, small amount of cyclohexene oxide is also observed at  $S/C \geq 50\ 000$  (Table 1, entries 4 and 5), and may be attributed to direct epoxidation of the olefinic bond. It is also worth mentioning the remarkable TON (>200 000) at  $S/C = 500\ 000$  (Table 1, entry 5), exclusively using  $O_2$  in total absence of reductant additives, while in literature TON of 250 is found for the same oxidation reaction, also using a magnetically recoverable porphyrin based catalyst.<sup>[47]</sup>

Next, the effect of the catalyst structure (**1a** and **2a**) on the conversion and selectivity was evaluated, taking aliquots from the reaction mixture, using a fixed S/C molar ratio of 500 000 and  $P(O_2) = 400$  KPa (Figure 4a,b).

From analysis of Figure 4a,b, we can observe that the substitution of fluorine by chlorine atoms on the *ortho*-positions of the copper-porphyrin phenyl ring did not significantly influenced the rate of cyclohexene oxidation and product distribution, after

4 h. Moreover, after  $\approx 20$  h no further evolution of the oxidation of cyclohexene was observed in both cases. This may be explained by catalyst degradation since the UV-vis spectra taken after 20 h did not show the presence of the typical Soret band ( $\approx 420$  nm) anymore (Figure S8, Supporting Information).

Next, we analyzed the performance of  $MNP@SiO_2$ -BNH-Cu-TDFPP **1b** and  $MNP@SiO_2$ -BNH-Cu-TDCPP **2b** catalysts in the oxidation of cyclohexene, using the optimized conditions obtained for the homogeneous catalytic system and the results are presented in Figure 5a,b).

Notably, nanomaterials **1b** and **2b** displayed a similar behavior concerning the rate of cyclohexene oxidation and product distribution, when compared to the homogeneous catalytic system. So, to evaluate the potentialities of these new magnetic oxidation catalysts regarding their recovering by action of an external magnetic field and reutilization in oxidation reactions, a set of experiments were carried out. First, the oxidation of cyclohexene using  $MNP@SiO_2$ -BNH-Cu-TDFPP **1b** or  $MNP@SiO_2$ -BNH-Cu-TDCPP **2b** as catalysts, was carried out under the reaction conditions described above for the homogeneous system. After 4 h conversions of 37% and 41%

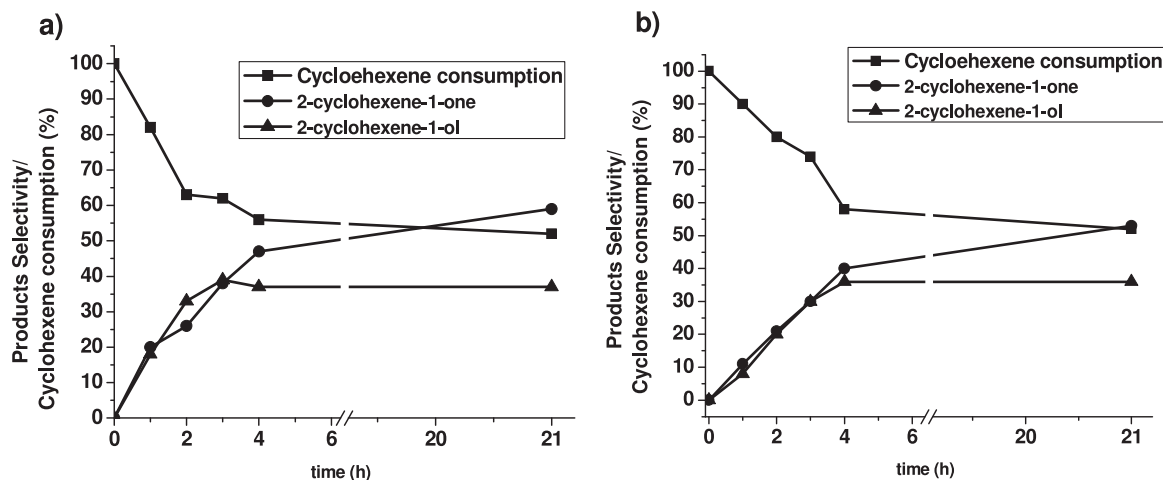


**Figure 5.** Cyclohexene oxidation products as a function of time using  $O_2$  (400 KPa) as oxidant and a)  $MNP@SiO_2$ -BNH-Cu-TDFPP **1b** and b)  $MNP@SiO_2$ -BNH-Cu-TDCPP **2b** as catalysts.

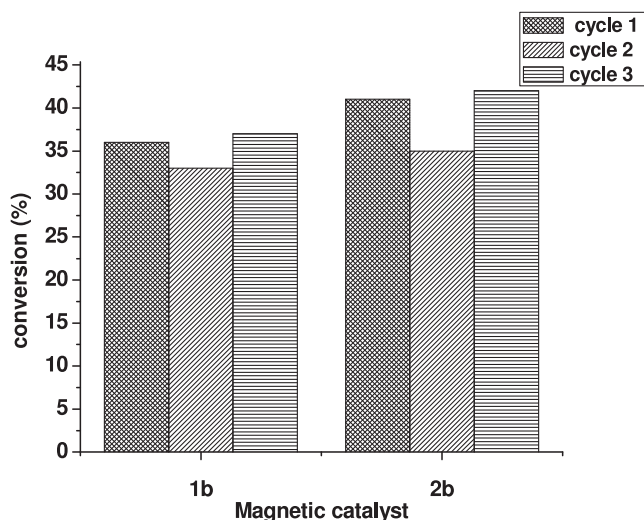


**Figure 6.** Conversion of cyclohexene using the magnetic catalysts **1b** or **2b** upon 3 cycles of reutilization. (Reaction Conditions: cyclohexene = 0.099 mol; catalyst = 0.197  $\mu$ mol of metalloporphyrin;  $T = 373$  K (100  $^{\circ}$ C);  $P(\text{O}_2) = 405$  KPa;  $t = 4$  h).

were obtained, respectively, as determined by GC-MS. Then, the reactor was cooled down to room temperature, depressurized and the magnetic catalysts were recovered by action of an external magnet. After washing the catalysts with dichloromethane (three times), two subsequent reactions were performed, under the same conditions and work-up, being the results plotted in **Figure 6**. The TON values were higher than 200 000 at 4 h of reaction (Tables S2–S5, Supporting Information).

From these results one can conclude that, contrarily to the homogeneous catalytic systems, where metalloporphyrin degradation was observed, in the heterogeneous system the catalysts could be reused, keeping their activity almost constant after three recycles (**Figure 6**).

In order to analyze the effect of time on the reaction rate beyond 4 h, additional experiments were performed. Using the above established reaction conditions (cyclohexene = 0.099 mol; catalyst **2b** = 0.197  $\mu$ mol;  $T = 373$  K (100  $^{\circ}$ C);  $P(\text{O}_2) = 405$  KPa;  $t = 4$  h), 48% cyclohexene conversion was observed. At this point, the reactor was cooled down to room temperature, depressurized and the magnetic catalyst was recovered by action of an external magnet. Then, more catalyst **2b** (0.197  $\mu$ mol) was added to the mixture and the reaction was continued for additional 4 h, after which no further cyclohexene conversion was observed (48%). Following this experiment, the reactor was again cooled down to room temperature, depressurized and the reaction mixture separated from the catalyst **2b** and collected from the reactor. Fresh cyclohexene (0.099 mol) was then added to the reactor containing catalyst **2b**, and 45% cyclohexene conversion was observed after 4 h of reaction. A possible reason for this occurrence may be that the products obtained from the cyclohexene oxidation reaction could inhibit the formation of additional oxidation products, but further studies are currently underway.

Moreover, to clarify the reaction mechanism, a similar cyclohexene oxidation reaction, using the  $\text{MNP}@SiO_2\text{-BNH-Cu-TDCPP}$  **2b** as catalyst, was performed, but in the presence

of 2,6-di-*tert*-butyl-4-methylphenol free-radical inhibitor. A conversion <2% was obtained after 21 h, which strongly corroborates the involvement of a thermolytically initiated radical mechanism, through single-electron-transfer of the Cu(II) based catalyst, as previously proposed in the literature.<sup>[60–63]</sup>

Also to evaluate the effect of the  $\text{MNP}@SiO_2$  support on cyclohexene oxidation, a blank reaction in the absence of metalloporphyrins was carried out and after 4 h a conversion <1% was obtained, which supports the contribution of the hybrid magnetic nanomaterials as catalyst to promote the radical oxidation reaction.

The scope of the reaction was extended to other substrates, namely, terpenes and thiophenol (whose oxidation products are reckoned as high added value products),<sup>[64–66]</sup> using the best conditions determined for the catalytic oxidation reaction performed in presence of supported copper-porphyrin catalyst  $\text{MNP}@SiO_2\text{-BNH-Cu-TDCPP}$  **2b**, with  $T = 373$  K (100  $^{\circ}$ C) and  $P(\text{O}_2) = 405$  KPa and the results are summarized in **Table 2**. Concerning  $\alpha$ -pinene and  $\beta$ -pinene oxidation, 45% and 15% conversions were obtained after 4 h, respectively (**Table 2**, entries 1 and 2). When  $\alpha$ -pinene was used as substrate, formation of  $\alpha$ -pinene oxide (**1**) (28%), verbenol (**2**) (33%) and hydroxy-limonene (**3**) (19%) was observed after 4 h (**Table 2**, entry 1). On other hand, the oxidation of  $\beta$ -pinene yielded pinocarvol (**4**) (20%), pinocarvone (**5**) (19%), and myrtenol (**6**) (58%) (**Table 2**, entry 2). In order to evaluate the potentiality of this greener oxidation approach to another type of compounds, the oxidation of thiophenol was also performed, reaching a conversion of 88% after 21 h with almost complete selectivity for the formation of diphenyl disulfide (98%; **Table 2**, entry 3).

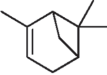
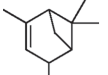
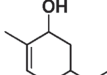
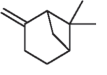
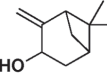
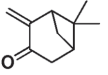
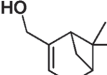
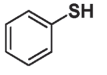
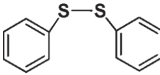
## 4. Conclusion

In summary, two new magnetically recoverable nanomaterials  $\text{MNP}@SiO_2\text{-BNH-Cu-TDFPP}$  (**2a**) and  $\text{MNP}@SiO_2\text{-BNH-Cu-TDCPP}$  (**2b**) were efficiently synthesized and were fully characterized by transmission electron microscopy, flame atomic absorption spectrometry, thermogravimetry,  $N_2$  sorption, and infrared spectroscopy, demonstrating an efficient anchoring.

Their precursory porphyrins TDFPP (**1a**) and TDCPP (**1b**) were evaluated as biomimetic catalysts in cyclohexene oxidation reaction using solely molecular oxygen, in total absence of reductants and solvents in TON as high as  $\approx 200$  000, using a substrate /catalyst ratio of 500 000/1 (cyclohexene conversion = 40%). Furthermore, magnetic hybrid nanomaterials **2a** and **2b** provided similar results in terms of catalytic activity, but were capable to promote the cyclohexene oxidation for several reutilization cycles without loss of activity or catalyst degradation. Experimental results corroborate the involvement of thermolytically initiated radical mechanism, through single-electron-transfer of the Cu(II) based catalyst.

The magnetic hybrid nanomaterial **2b** was further tested, under similar reaction conditions, as catalyst in the oxidation of several other substrates, namely,  $\alpha$ -pinene,  $\beta$ -pinene, and thiophenol, demonstrating higher catalytic activity toward  $\alpha$ -pinene than  $\beta$ -pinene. On the other hand, oxidation of thiophenol gave exclusively diphenyl disulfide in 98%.

**Table 2.** Oxidation reactions using magnetic catalyst MNP@SiO<sub>2</sub>-BNH-Cu-TDCPP **2b** (in parenthesis are the percentages after 21 h).

| Subst  | Entry | Time [h] | Conv. [%] | Product selectivity [%]  |  |  |                   |
|--|-------|----------|-----------|--|--|--|-------------------|
| <br><b>α-pinene</b>   | 1     | 4 (21)   | 45 (57)   | <br><b>1</b><br>28 (8)  | <br><b>2</b><br>33 (27) | <br><b>3</b><br>19 (34) | Others<br>19 (22) |
| <br><b>β-pinene</b>   | 2     | 4 (21)   | 15 (34)   | <br><b>4</b><br>20 (25) | <br><b>5</b><br>19 (-)  | <br><b>6</b><br>58 (52) | Others<br>3 (23)  |
| <br><b>Thiophenol</b> | 3     | 4 (21)   | 24 (88)   | <br>98 (98)             | Others<br>2 (2)  | -  | -                 |

The above studies are pertinent with regard to industrial processes, and allylic oxidation is a powerful synthetic transformation, reason why a reusable magnetic hybrid copper porphyrin based catalytic system such as the one here reported, using solely molecular oxygen, without addition of any coreductant and/or other additives on the oxidation of olefins, under milder conditions, may possess many advantages over reported reagents and catalysts, which rely on toxic metals and/or toxic/costly oxidants.

## 5. Experimental Section

**Materials and Methods:** All chemical materials were purchased from Aldrich having the highest grade available and used as-received. Solvents were purified by standard methods. The MALDI-TOF MS data were acquired using a Bruker Daltonics flex Analysis apparatus. <sup>1</sup>H NMR spectra were recorded on a 400 MHz Bruker-Amx and TMS was used as standard. UV-vis absorption spectra were recorded on a Hitachi U-2010. TEM analyses were carried out on a Philips CM 200 operating at an accelerating voltage of 200 kV. The TEM samples were prepared in isopropyl alcohol, at room temperature, and then placed onto holey carbon-covered copper grids to dry before analysis. The size distributions were determined through a manual analysis of enlarged images with Imagetool sware Version 3.0 to obtain a statistical size distribution and a mean diameter by curve fitting using Gaussian function. The metal content in all MNP@SiO<sub>2</sub>-BNH-Cu-TDCPP and MNP@SiO<sub>2</sub>-BNH-Cu-TDFPP was measured by FAAS using an Atomic Absorption Spectrophotometer Shimadzu AA-6300, using quartz cells. Thermogravimetric analyses were made in air using a TG-DSC Setsys Evo16 instrument (Setaram) with a heating rate of 10 K min<sup>-1</sup> to a maximum temperature of 800 °C. Nitrogen adsorption measurements were carried out with a Micromeritics ASAP 2010 apparatus. Prior to analysis, all samples were pre-treated for 1 h at 333 K (60 °C) and then at 383 K (110 °C) for 4 h under vacuum. The infrared spectra were obtained using a FTIR Nexus 670 Nicolet spectrometer. The samples were pressed into thin wafers (20–25 mg cm<sup>-2</sup>) and heated in an IR glass cell from room temperature up to 323 K (150 °C) (heating rate of 5 K min<sup>-1</sup>) for 1.5 h, under vacuum (10 Pa) before spectra acquisition in transmission

mode. 64 scans with a resolution of 4 cm<sup>-1</sup> were collected for each spectrum. The oxidation products were collected and analyzed by GC-MS, using a Shimadzu GC-17A, gas chromatograph and a Shimadzu 14B/QP5050A GC/MS system with a PBX5 column (5% phenyl, 95% polysilphenylenesiloxane), and helium as carrier gas. The analyses were performed using the following conditions: initial temperature 313 K (40 °C), rate 10 K min<sup>-1</sup>, final temperature 473 K (200 °C) and gas flow of 1.41 mL min<sup>-1</sup>. Conversion and selectivity were calculated based on peak areas of GC calibrated with an internal standard (p-xylene). The validity of the identification and quantitation of the GC peaks was verified by comparison of the mass spectra and gas chromatographic retention times with those of the authentic compounds.

**Synthesis of Metalloporphyrins and Hybrid Magnetic Materials:** The *meso*-tetra(2,6-difluorophenyl)porphyrin (TDFPP; **1**) and *meso*-tetra(2,6-dichlorophenyl)porphyrin (TDCPP; **2**) were synthesized, purified, and characterized following our recent developments of nitrobenzene method with presence of NaY<sup>49</sup> and also the water/microwave method.<sup>50</sup> The TDFPP (**1**) was obtained with yield of 9% (water/microwave method) and 21% (nitrobenzene/NaY method). The TDCPP (**2**) was isolated with yield of 3% (water/microwave method) and 7.5% (nitrobenzene/NaY method). The characterization data are in agreement with the literature.<sup>49,50</sup>

**Synthesis of BNO<sub>2</sub>-Cu-TDFPP (**1a**):** To a round bottom 1 L flask containing 5,10,15,20-tetra(2,6-difluorophenyl)porphyrin (TDFPP) (500 mg, 0.66 mmol) dissolved in chloroform (500 mL), a solution of copper nitrate trihydrate (0.32 g, 1.32 mmol) in acetic anhydride/acetic acid (50/10 mL) was added. The reaction was left stirring at 333 K (60 °C), along 7 h. The solution was then concentrated under vacuum and washed with a saturated solution of sodium bicarbonate (two times), distilled water (one time) and dried with anhydrous sodium sulfate. After solvent evaporation, the crude was purified by silica gel column chromatography using dichloromethane: *n*-hexane (1:1) as eluent. The copper(II) 2-nitro-5,10,15,20-tetra(2,6-difluorophenyl)porphyrinate (BNO<sub>2</sub>-Cu-TDFPP; **1a**) was isolated in 89% yield (506 mg). MS (MALDI-TOF): *m/z* = 864.070 [M]<sup>+</sup> calcd. for C<sub>44</sub>H<sub>19</sub>F<sub>8</sub>N<sub>5</sub>O<sub>2</sub>Cu 864.065. Anal. calcd. for C<sub>44</sub>H<sub>19</sub>F<sub>8</sub>N<sub>5</sub>O<sub>2</sub>Cu: C 61.07, H 2.24, N = 8.07; found: C 61.08, H 2.21, N 8.09.

**Synthesis of BNO<sub>2</sub>-Cu-TDCPP (**2a**):** The procedure described above was used, but with 5,10,15,20-tetra(2,6-dichlorophenyl)porphyrin (TDCPP; 400 mg, 0.45 mmol) and stirring at 323 K (50 °C) along 24 h. After work-up, the copper(II) 2-nitro-5,10,15,20-tetra(2,6-dichlorophenyl)porphyrinate (BNO<sub>2</sub>-Cu-TDCPP) was isolated in 76% yield (336 mg).

MS (MALDI-TOF):  $m/z = 995.700$   $[M]^+$  calcd. for  $C_{44}H_{19}Cl_8N_5O_2Cu$  995.830. Anal. calcd. for  $C_{44}H_{19}Cl_8N_5O_2Cu$ : C 53.07, H 1.89, N 7.07; found: C 53.02, H 1.92, N 7.07.

**Synthesis of Magnetic Nanoparticles (MNP):** Magnetite nanoparticles were prepared, according to a procedure previously reported by some of us.<sup>[53]</sup> A mixture of aqueous solution of  $FeCl_3$  (10 mL, 1 M) and a 2 M HCl solution of  $FeCl_2$  (2.5 mL, 2 M) was added to  $NH_4OH$  (250 mL, 1 M) under mechanical stirring (10 000 rpm, Ultra-Turrax T18 Homogenizer, IKA Works). After 30 min the MNP were magnetically recovered and washed with distilled water ( $3 \times 250$  mL). Then, the MNP were dispersed again in distilled water (250 mL) and oleic acid (2 mL, 7 mmol), diluted in acetone (5 mL), was added dropwise under vigorous mechanical stirring for 30 min. The resulting precipitate was magnetically separated, washed with acetone (three times, 25 mL) and redissolved in cyclohexane (15 mL). The final solution was centrifuged (2000 rpm, 30 min) to remove the nonstabilized particles and was stocked under air. After solvent evaporation a stock solution containing 72 mg of MNP/mL of cyclohexane was obtained.

**Coating Magnetic Nanoparticles with Silica (MNP@SiO<sub>2</sub>):** The silica coating was obtained by means of reverse microemulsion process.<sup>[54]</sup> Igepal CO-520 (178.4 g), magnetite (800 mg; 11.1 mL of stock solution in cyclohexane), and ammonium hydroxide (29%; 38 mL) were dispersed in cyclohexane (2.8 L). Then, tetraethyl orthosilicate (TEOS; 30.8 mL) was added dropwise and the mixture was kept under slow mechanical stirring (300 rpm) along 16 h. The solid was precipitated with methanol ( $\approx 250$  mL), recovered by centrifugation (7000 rpm, 30 min) and washed with ethanol (three times). Finally, the solid material was dried open air for 24 h, at room temperature, and then calcined in the oven at 773 K (500 °C) for 2 h. Typically, 5.40 g of magnetic nanoparticles coated with silica (MNP@SiO<sub>2</sub>) were obtained.

**Preparation of Amine-Functionalized Magnetic Nanoparticles (MNP@SiO<sub>2</sub>-NH<sub>2</sub>):** MNP@SiO<sub>2</sub> (1 g) was mixed with 3-aminopropyltriethoxysilane (APTES; 0.5 mL) in dry toluene at temperature reflux for 2 h. Then, the amine-functionalized solid (MNP@SiO<sub>2</sub>-NH<sub>2</sub>) was washed with toluene, separated by centrifugation, and dried at 273 K (100 °C) for 20 h.

**Anchoring of Metalloporphyrins BNO<sub>2</sub>-Cu-TDFPP (1a) and BNO<sub>2</sub>-Cu-TDCPP (2a) to MNP@SiO<sub>2</sub>-NH<sub>2</sub>:** A mixture of MNP@SiO<sub>2</sub>-NH<sub>2</sub> (1.5 g), metalloporphyrin (0.33 mmol) and cesium carbonate (1.9 mmol; 388 mg) in dry DMF (150 mL) was heated at 423 K (150 °C) along 24 h. The product was magnetically collected and washed several times with acetonitrile, ethyl acetate, and dichloromethane to rinse away excess of BNO<sub>2</sub>-Cu-TDFPP (1a) or BNO<sub>2</sub>-Cu-TDCPP (2a). The final materials 1b and 2b were dried under vacuum for 24 h.

**General Procedure for Catalytic Oxidations:** In a typical reaction, the reactor was loaded with catalyst (0.197  $\mu$ mol) and the desired amount of substrate and then charged with molecular oxygen (400 kPa). The reaction was maintained at 373 K (100 °C) for 4 h under magnetic stirring (700 rpm) using Teflon-coated magnetic stir bar. After this period, the reactor was cooled to room temperature, opened to air and an aliquot was taken, dissolved in dichloromethane, and analyzed by gas chromatography. For magnetic catalyst recovery, a permanent magnet was placed on the reactor wall.

**Homogeneous Catalysis:** Using the above described method the typical reaction conditions were: metalloporphyrin 1a or 2a (0.197  $\mu$ mol) and cyclohexene (99 mmol; 10 mL) used as substrate and solvent.

**Heterogeneous Catalysis:** The heterogeneous oxidation reactions were optimized for each substrate used and the best reaction conditions are presented below: Cyclohexene/catalyst/ = 500 000/1 (cyclohexene = 99 mmol, 10 mL; catalyst = 0.197  $\mu$ mol of porphyrin onto 13 mg of magnetic material 1b); Cyclohexene/Catalyst = 500 000/1 (cyclohexene = 99 mmol, 10 mL; catalyst = 0.197  $\mu$ mol of porphyrin onto magnetic material 2b (39 mg); Pinene/catalyst = 250 000/1 ( $\beta$ -pinene or  $\alpha$ -pinene = 50 mmol, 7.9 mL; catalyst = 0.197  $\mu$ mol of porphyrin onto 39 mg magnetic material 2b); Thiophenol/Catalyst = 250 000/1 (Thiophenol = 50 mmol, 7.9 mL; catalyst = 0.197  $\mu$ mol of porphyrin onto 39 mg magnetic material 2b).

## Supporting Information

Supporting Information is available from the Wiley Online Library or from the author.

## Acknowledgements

The Coimbra Chemistry Centre and Centro de Química Estrutural were supported by the Fundação para a Ciência e a Tecnologia (FCT) (Portuguese Foundation for Science and Technology), through Project Nos. PEst-OE/QUI/UI01313/2014 and UID/QUI/00100/2013, respectively. The authors are thankful to FCT, FEDER – European Regional Development Fund through the COMPETE Programme (Operational Programme for Competitiveness) for funding. C.A.H. is grateful for his Ph.D. grant SFRH/BD/84146/2012, A.F. is grateful for his post-doctoral grant SFRH/BPD/91397/2012, and M.J.F.C. is grateful for his post-doctoral grant SFRH/BPD/99698/2014, all supported by FCT-Portugal. NMR data were collected at the UC-NMR facility which is supported in part by FEDER and FCT through Grant Nos. REEQ/481/QUI/2006, RECI/REQ-QFI/0168/2012, CENTRO-07-CT62-FEDER-002012, and Rede Nacional de Ressonância Magnética Nuclear (RNRMN). Finally, the authors thank Prof. Pedro K. Kiyohara from the Institute of Physics at USP for the TEM analysis.

Received: December 15, 2015

Published online: February 12, 2016

- [1] G. H. Loew, D. L. Harris, *Chem. Rev.* **2000**, *100*, 407.
- [2] P. R. Ortiz-de-Montellano, J. J. De Voss, *Nat. Prod. Rep.* **2002**, *19*, 477.
- [3] J. Bernadou, B. Meunier, *Adv. Synth. Catal.* **2004**, *346*, 171.
- [4] H.-B. Ji, X.-T. Zhou, in *Biomimetic Homogeneous Oxidation Catalyzed by Metalloporphyrins with Green Oxidants, Biomimetics Learning from Nature* (Ed: A. Mukherjee), Intech, Rijeka, **2010**, Ch. 7.
- [5] L. R. Milgrom, *The Colours of Life: An Introduction to the Chemistry of Porphyrins and Related Compounds*, Oxford University Press, New York **1997**.
- [6] B. Meunier, A. Robert, G. Pratviel, J. Bernadou, in *The Porphyrin Handbook* (Eds: K. M. Kadish, K. M. Smith, R. Guilard), Academic Press, San Diego, CA **2000**, pp. 119–187.
- [7] L. Que, W. B. Tolman, *Nature* **2008**, *455*, 333.
- [8] D. Mansuy, *C. R. Chim.* **2007**, *10*, 392.
- [9] S. L. H. Rebelo, M. M. Pereira, M. M. Q. Simões, M. Graça P. M. S. Neves, J. A. S. Cavaleiro, *J. Catal.* **2005**, *234*, 76.
- [10] C.-M. Che, J.-S. Huang, *Chem. Commun.* **2009**, 3996.
- [11] G. B. Shul'pin, *J. Mol. Catal. A: Chem.* **2002**, *189*, 39.
- [12] *Metalloporphyrins in Catalytic Oxidations* (Ed. R. A. Sheldon), Marcel Dekker, New York **1994**.
- [13] M. J. F. Calvete, M. Silva, M. M. Pereira, H. D. Burrows, *RSC Adv.* **2013**, *3*, 22774.
- [14] J. Y. Lee, O. K. Farha, J. Roberts, K. A. Scheidt, S. T. Nguyen, J. T. Hupp, *Chem. Soc. Rev.* **2009**, *38*, 1450.
- [15] S. Nakagaki, G. K. B. Ferreira, A. L. Marçal, K. J. Ciuffi, *Curr. Org. Synth.* **2014**, *11*, 67.
- [16] Z. Shi, C. Zhang, C. Tang, N. Jiao, *Chem. Soc. Rev.* **2012**, *41*, 3381.
- [17] T. Punniyamurthy, S. Velusamy, J. Iqbal, *Chem. Rev.* **2005**, *105*, 2329.
- [18] Q. Liu, C.-C. Guo, *Sci. China* **2012**, *55*, 2036.
- [19] W. Nam, S.-Y. Oh, Y. J. Sun, J. Kim, W.-K. Kim, S. K. Woo, W. Shin, *J. Org. Chem.* **2007**, *68*, 7903.
- [20] K. A. Srinivas, A. Kumar, M. S. Chauhan, *Chem. Commun.* **2002**, 2456.
- [21] G. Grigoropoulou, J. H. Clark, J. A. Elings, *Green Chem.* **2003**, *5*, 1.

- [22] S. L. H. Rebelo, M. M. Q. Simoes, M. G. P. M. S. Neves, A. M. S. Silva, J. A. S. Cavaleiro, A. F. Peixoto, M. M. Pereira, M. R. Silva, J. A. Paixao, A. M. Beja, *Eur. J. Org. Chem.* **2004**, 23, 4778.
- [23] I. Tabushi, K. Morimitsu, *Tetrahedron Lett.* **1986**, 27, 51.
- [24] I. Tabushi, A. Yazaki, *J. Am. Chem. Soc.* **1981**, 103, 7370.
- [25] F. Bedioui, J. Devynck, C. Bied-Charreton, *J. Mol. Catal. A: Chem.* **1996**, 113, 3.
- [26] J. E. Lyons, P. E. Ellis, H. K. Myers, *J. Catal.* **1995**, 155, 59.
- [27] J. Haber, L. Matachowski, K. Pamin, J. Poltowicz, *J. Mol. Catal. A: Chem.* **2003**, 198, 215.
- [28] W. J. Yang, C. C. Guo, N. Y. Tao, J. Cao, *Kinet. Catal.* **2010**, 51, 194.
- [29] C. Sun, B. Hu, Z. Liu, *Chem. Eng. J.* **2013**, 232, 96.
- [30] J. T. Groves, R. Quinn, *J. Am. Chem. Soc.* **1985**, 107, 5790.
- [31] W. Liu, Q. Liu, C. C. Guo, *J. Chem. Indust. Eng. (China)* **2005**, 59, 1537.
- [32] Y. F. Li, C. C. Guo, X. H. Yan, Q. Liu, *J. Porphy. Phthalocya.* **2006**, 10, 942.
- [33] C. C. Guo, W. J. Yang, Y. L. Ming, *J. Mol. Catal. A: Chem.* **2005**, 226, 279.
- [34] H. Arakawa, M. Aresta, J. N. Armor, M. A. Barteau, E. J. Beckman, A. T. Bell, J. E. Bercaw, C. Creutz, E. Dinmijus, D. A. Dixon, K. Domen, D. L. Dubois, J. Eckert, E. Fujita, D. H. Gibson, W. A. Goddard, D. Wayne Goodman, J. Keller, G. J. Kubas, H. H. Kung, J. E. Lyons, L. E. Manzer, T. J. Marks, K. Morokuma, K. M. Nicholas, R. Periana, L. Que, J. Rostrup-Nielsen, W. M. H. Sachtler, L. D. Schmidt, A. Sen, G. A. Somorjai, P. C. Stair, B. R. Stults, W. Tumas, *Chem. Rev.* **2001**, 101, 953.
- [35] C.-J. Liu, W.-Y. Yu, S.-G. Li, C.-M. Che, *J. Org. Chem.* **1998**, 63, 7364.
- [36] G. S. Machado, K. A. D. F. Castro, O. J. Lima, E. J. Nassar, K. J. Ciuffi, S. Nakagaki, *Colloid. Surf. A* **2009**, 349, 162.
- [37] H. C. Sacco, Y. Iamamoto, J. R. Lindsay-Smith, *J. Chem. Soc., Perkin Trans. 2* **2001**, 181.
- [38] X.-Q. Yu, J.-S. Huang, W.-Y. Yu, C.-M. Che, *J. Am. Chem. Soc.* **2000**, 122, 5337.
- [39] S. Tangestaninejad, M. Moghadam, *Synth. Commun.* **1998**, 28, 427.
- [40] M. Moghadam, V. Mirkhani, S. Tangestaninejad, I. Mohammadpoor-Baltork, A. A. Abbasi-Larki, *Appl. Catal. A* **2008**, 349, 177.
- [41] S. Nakagaki, F. L. Benedito, F. Wypych, *J. Mol. Catal. A: Chem.* **2004**, 217, 121.
- [42] N. Bizaia, E. H. Faria, G. P. Ricci, P. S. Calefi, E. J. Nassar, K. A. D. F. Castro, S. Nakagaki, K. J. Ciuffi, R. Trujillano, M. A. Vicente, A. Gil, S. A. Koril, *ACS Appl. Mater. Interfaces* **2009**, 1, 2667.
- [43] P. M. Uberman, N. J. S. Costa, K. Philippot, R. C. Carmona, A. A. Dos Santos, L. M. Rossi, *Green Chem.* **2014**, 16, 4566.
- [44] M. Shokouhimehr, Y. Piao, J. Kim, Y. Jang, T. Hyeon, *Angew. Chem. Int. Ed.* **2007**, 46, 7039.
- [45] C.-X. Liu, Q. Liu, C.-C. Guo, Z. Tan, *J. Porphy. Phthalocya.* **2010**, 14, 825.
- [46] J. S. Santos, A. L. Faria, P. M. S. Amorin, F. M. La Luna, K. L. Caiado, D. O. C. Silva, P. P. C. Sartoratto, M. D. Assis, *J. Braz. Chem. Soc.* **2012**, 23, 1411.
- [47] M. Bagherzadeh, A. Mortazavi-Manesh, *J. Coord. Chem.* **2015**, 68, 2347.
- [48] G. M. Ucoski, G. S. Machado, G. F. Silva, F. S. Nunes, F. Wypych, S. Nakagaki, *J. Mol. Catal. A: Chem.* **2015**, 408, 123.
- [49] M. Silva, A. Fernandes, S. S. Bebiano, M. J. F. Calvete, M. F. Ribeiro, H. D. Burrows, M. M. Pereira, *Chem. Commun.* **2014**, 6571.
- [50] C. A. Henriques, S. M. A. Pinto, G. L. B. Aquino, M. Pineiro, M. J. F. Calvete, M. M. Pereira, *ChemSusChem* **2014**, 7, 2821.
- [51] C. A. Henriques, S. M. A. Pinto, M. Pineiro, J. Canotilho, M. E. S. Eusébio, M. M. Pereira, M. J. F. Calvete, *RSC Adv.* **2015**, 5, 64902.
- [52] R. Luguya, L. Jaquinod, F. R. Fronczek, A. G. H. Vicente, K. M. Smith, *Tetrahedron* **2004**, 60, 2757.
- [53] L. M. Rossi, L. L. R. Vono, F. P. Silva, P. K. Kiyohara, E. L. Duarte, J. R. Matos, *Appl. Catal. A* **2007**, 330, 139.
- [54] M. J. Jacinto, Pedro K. Kiyohara, S. H. Masunaga, R. F. Jardim, L. M. Rossi, *Appl. Catal. A* **2008**, 338, 52.
- [55] J. Muzart, *Tetrahedron* **2009**, 65, 8313.
- [56] Z. Bohstrom, I. Rico-Lattes, K. Holmberg, *Green Chem.* **2010**, 2, 1861.
- [57] S. Cohen, S. Kozuch, C. Hazan, S. Shaik, *J. Am. Chem. Soc.* **2006**, 128, 11028.
- [58] P. Jin, Z. H. Zhao, Z. P. Dai, D. H. Wei, M. S. Tang, X. Y. Wang, *Catal. Today* **2011**, 175, 619.
- [59] L. K. Stultz, M. H. V. Huynh, R. A. Binstead, M. Curry, T. J. Meyer, *J. Am. Chem. Soc.* **2000**, 122, 5984.
- [60] Y. Li, X.-T. Zhou, H.-B. Ji, *Cat. Commun.* **2012**, 27, 169.
- [61] S. E. Allen, R. R. Walvoord, R. Padilla-Salinas, M. C. Kozlowski, *Chem. Rev.* **2013**, 113, 6234.
- [62] X. Zhang, R. Yi, T. Chen, S. Ni, G. Wang, L. Yu, *Sci. J. Frontier Chem. Dev.* **2013**, 3, 25.
- [63] F. P. Silva, M. J. Jacinto, R. Landers, L. M. Rossi, *Catal. Lett.* **2011**, 141, 432.
- [64] U. Neuenschwander, F. Guignard, I. Hermans, *ChemSusChem* **2010**, 3, 75.
- [65] J. L. F. Monteiro, C. O. Veloso, *Top. Catal.* **2004**, 27, 1.
- [66] A. Corma, P. Concepción, M. Boronat, M. J. Sabater, J. Navas, M. J. Yacaman, E. Larios, A. Posadas, M. A. López-Quintela, D. Buceta, E. Mendoza, G. Guilera, A. Mayoral, *Nat. Chem.* **2013**, 5, 775.